Electron Scattering and Nuclear Charge Distributions

D. G. RAVENHALL

Department of Physics, University of Illinois

I. INTRODUCTION

THE scattering of high-energy electrons by nuclei, and the information it gives about nuclear charge distributions has already been extensively reviewed.[1–3] Electron scattering is the source of the most accurate and detailed information about nuclear charge size, and we wish to dwell on the assumptions and approximations made in the analysis of the experiments. We do not list exhaustively the results obtained, but quote from them to illustrate the rather different approaches adopted for various regions of the periodic table.

Apart from some early exploratory work[4,5] the experiments used are entirely those of Hofstadter and his colleagues at Stanford.[6] The experimental methods are not discussed; we consider only the end product, which for elastic scattering is a differential cross section which decreases very rapidly with increasing angle. From the detailed shape of this curve information is extracted about nuclear change distributions.

II. THEORY

In elastic scattering the electron interacts with the static Coulomb field of the nuclear charge distribution. The scattering can be calculated by the simple Born approximation; this provides an easy understanding of the salient features of the process, and when used carefully it is a very helpful guide to more exact calculation. For the differential cross section this gives the familiar result

$$\frac{d\sigma}{d\Omega}=\left(\frac{2\gamma}{q^2}\right)^2 k^2\cos^2\tfrac{1}{2}\theta\,|F(q)|^2, \tag{1}$$

where q is the recoil wave number for the process, of magnitude $2k\sin\frac{1}{2}\theta$, where k is the electron wave number and θ is the scattering angle. The factor $\cos^2\frac{1}{2}\theta$ is the only manifestation of the electron spin. The effect of finite size is contained in the factor $|F(q)|^2$. Here $F(q)$ is the Fourier transform of the charge distribution $\rho(r)$,

$$F(q)=\int d^3r\rho(r)e^{iq\cdot r}, \tag{2}$$

in this case normalized to unity for zero q. It is commonly called the "form factor," because of its similarity to the corresponding quantity occurring in x-ray diffraction.

As a function of angle the differential cross section (1) has, close to the forward direction, the familiar Rutherford $\sin^{-4}\frac{1}{2}\theta$ behavior; at large angles this relatively slowly varying part is modified by $F(q)$, which in most cases of interest decreases rapidly with increasing angle, the exact manner of the decrease depending sensitively on $\rho(r)$. The method used for extracting $\rho(r)$ from the experiments is essentially to compare the experimental cross section with the theoretical cross section for scattering from a point (i.e., with $F=1$) and to try to find forms for ρ, with over-all character suggested by other knowledge of the particular nucleus being examined, whose Fourier transforms reproduce the observed reduction from point scattering.

The actual scattering process is not as simple as the outline suggests. Even with the assumption that the interaction between electrons and nuclei is entirely electromagnetic, the fact that it is possible for the electrons to excite the nucleus means that there are other contributions to the scattering besides that caused by the static Coulomb potential. In terms of an optical model for elastic scattering, there is a contribution to the real potential arising from virtual excitation of the nucleus; Schiff's calculation of it[7] uses sum rules to include all nuclear excitations, and in this approximation he relates it to the (unknown) correlation function for pairs of protons in the nucleus. He finds an effect on the scattering of order e^2/hc compared with the main, Coulomb part. There must also be an imaginary potential to describe the decrease in flux of elastically scattered electrons due to the inelastic scattering. This is related to the total inelastic cross section, and is therefore calculated separately. Valk[8] finds that for hydrogen and deuterium the effect is rather small (at most a few percent) and a similar con-

[1] R. Hofstadter, Revs. Modern Phys. **28**, 214 (1956), gives a compilation of results obtained up to that time.
[2] R. Hofstadter, Ann. Revs. Nuclear Sci. **7**, 231 (1957), contains a complete account of the theory of electron scattering.
[3] K. W. Ford and D. L. Hill, Ann. Revs. Nuclear Sci. **5**, 25–72 (1955), deals with all methods for examining nuclear charge distributions, and includes a description of the earlier results of electron scattering.
[4] Lyman, Hanson, and Scott, Phys. Rev. **84**, 626 (1951).
[5] Pidd, Hammer, and Raka, Phys. Rev. **92**, 436 (1953).
[6] See references 1 and 2 for a complete bibliography.
[7] L. I. Schiff, Nuovo cimento **5**, 1223 (1957), lists and discusses the earlier work on this topic. A calculation which avoids the use of the closure relation for the intermediate states has been made for deuterium by H. S. Valk and B. J. Malenka, Phys. Rev. **104**, 800 (1956).
[8] H. S. Valk, Nuovo cimento **6**, 173 (1957).

clusion can be reached for heavier nuclei. The relative contributions of the various terms depend sensitively on the appropriate form factors, however, and these calculations are all too crude to give more than a rough estimate of them. It would be desirable to have a detailed calculation of these effects for a nucleus whose dominant modes of excitation are relatively well understood, so that we could be completely sure of their unimportance in the analysis of the elastic scattering. Such a calculation does not as yet exist. It is reassuring, however, that if we neglect them entirely, and assume only the Coulomb potential, we obtain a completely consistent fit with experiments at various energies using the same (energy independent) $\rho(r)$, so that there is no strong evidence that they are present to any appreciable extent in the experiments carried out up to now.

The other, and by now well-known, defect of the analysis as outlined is that the Born approximation as it stands is not accurate enough for any except the lightest nuclei. Although the ratio $V_C(0)/E$ is never more than about one-tenth for the situations in which we are interested, this is not the correct criterion for applicability of the Born approximation, because of the long range of the potential. The practical remedy is very simple, at least for charge distributions which are spherically symmetric: one makes a (perforce numerical) partial wave analysis of the Dirac equation, in a manner that has been known for many years.[9] There are some rather thorny computational problems which arise in doing this, all originating in the along-range nature of the Coulomb field.[10] But in practice the procedure can be reduced to that of simply feeding to a big computer a given charge distribution, and waiting for a short time until a differential cross-section emerges.[11] The comforting aspect of this physically rather unsatisfying procedure is that there is complete quantitative agreement among the various groups who have independently made such computations: Hill and Ford[3]; Brenner, Brown, and Elton[12]; Glassgold[13]; and the Stanford group.[1,2]

It is perhaps not entirely surprising that the differential cross sections which follow from the partial-wave analysis have many features in common with the corresponding Born approximation results. Figure 1, shows that, except for the first diffraction dip in heavy nuclei the whole difference can be encompassed by a filling in of the zeros of the Born approximation, and a shifting of the diffraction structure to smaller angles. The extent of these effects increases with increasing Z. These changes have been understood qualitatively for a long time as being due to the distortion of the incident electron wave in the slowly varying tail of the Coulomb potential and the concomitant increase in the electron's wave number.[14] This approach has now been carried to the stage of giving quite accurate agreement with the partial-wave answers for the elastic scattering.[15] The Coulomb potential is divided into the potential of a very smooth charge distribution $\rho_s(r)$ with the same total charge, plus the remainder; the latter is now a short range potential ΔV which contains all of the high Fourier components of the original potential. The scattering due to ΔV is calculated by perturbation theory,

$$\Delta f(\theta)=\int \varphi^{(-)*}(\mathbf{r})\Delta V\varphi^{(+)}(\mathbf{r})d^3r, \qquad (3)$$

using an analytic approximation to the wave functions

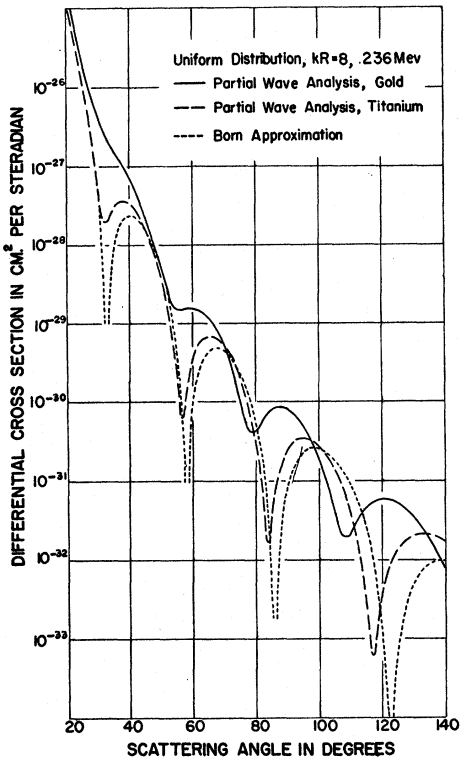

FIG. 1. Differential cross sections for scattering at 236 Mev by a uniform charge distribution $kR=8$ for gold ($Z=79$) and titanium ($Z=23$). This illustrates the apparent effects of the phase shift analysis in filling in the zeros of the Born approximation cross section and shifting them to smaller angles.

[9] N. F. Mott and H. S. W. Massey, *The Theory of Atomic Collisions* (Clarendon Press, Oxford, 1949), second edition, p. 78.
[10] Yennie, Ravenhall, and Wilson, Phys. Rev. **95**, 500 (1954).
[11] All of the numerical partial-wave calculations made by the Stanford group, after those reported in reference 10, were performed on the computer Univac at the University of California Radiation Laboratory at Livermore. We wish to thank the authorities of this Laboratory, and particularly Dr. Sidney Fernbach, for making Univac available to us, and also the many people at Livermore whose assistance has enabled us to use it.
[12] Brenner, Brown, and Elton, Phil. Mag. **45**, 524 (1954); G. E. Brown and L. R. B. Elton, Phil. Mag. **46**, 164 (1955).
[13] A. E. Glassgold, Phys. Rev. **98**, 1360 (1955).
[14] Yennie, Ravenhall, and Downs, Phys. Rev. **98**, 277(A) (1955).
[15] Yennie, Ravenhall, and Tiemann (paper in preparation). A different approach has been adopted by Schiff, Phys. Rev. **103**, 443 (1956), who sums the Born series analytically for the scattering amplitude, using a stationary phase approximation. The two methods are very similar in many ways.

φ for scattering under the influence of $\rho_s(r)$. The *scattering* due to $\rho_s(r)$ decreases very rapidly with angle, so that finally the only contribution to the scattering amplitude is (3), where the functions $\varphi(r)$ are actually the distorted waves just described. The answer is thus very similar to that of the Born approximation, with the modification previously mentioned. We can now use the ideas of the Born approximation, for instance the connection between scattering at large q and the presence of the corresponding Fourier components of ρ, if not with impunity, at least with some success.

III. RESULTS

From the analysis of scattering from the proton[16] we use only the conclusion that its charge distribution is relatively smooth, with a root-mean-square radius of about 0.8×10^{-13} cm.

Deuterium

The model to be used is provided by the well-explored Schrödinger equation for the relative motion of the neutron and proton, with static potentials obtained by fitting the low-energy properties of this system.[17] The effects of the deuteron magnetic dipole and electric quadrupole moments are appreciable only at the largest q values attained, and are not very important even there.[18] The theory as applied to electron scattering is thus quite simple. The rather disappointing feature of the results is that the quite wide variety of potential shapes that have been tried (Yukawa, repulsive core, etc.) give very similar electron-scattering differential cross sections, so that it has not been possible to conclude very much about them. This is illustrated in Fig. 2. The result that has proved useful is that it is not possible to fit the experimental results with any of these static-potential models unless allowance is made for the finite size of the proton; the assumption must be made that $|\psi_D(r)|^2$ describes the distribution in space of the centers of mass of neutron and proton; the actual charge distribution is larger than this because the proton itself has a finite extension (and the neutron has zero extension).[19] With the assumption of sizes as for free nucleons, the agreement with the Schrödinger theory is very good, as can be seen in Fig. 3.

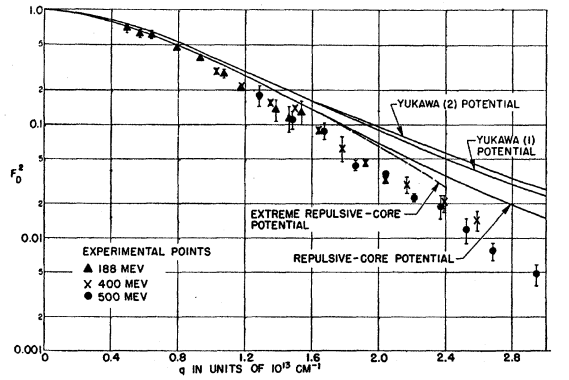

FIG. 2. Experimental and theoretical results for deuterium, expressed as $|F(q)|^2$ *vs* q^2, assuming zero extension for the proton. The points are experimental data obtained at various energies up to 400 Mev, and the neutron-proton potentials used in deriving the theoretical curves are chosen to give the correct low-energy properties of the two-nucleon system.

[16] E. E. Chambers and R. Hofstadter, Phys. Rev. **103**, 1454 (1956).
[17] V. Z. Jankus, Phys. Rev. **102**, 1586 (1956).
[18] J. A. McIntyre and S. Dhar, Phys. Rev. **106**, 1074 (1957).

Helium

At this stage, since there is not such a well-explored model to utilize, and the analysis must therefore be a little more experimental, a word should be said about the fitting procedure.

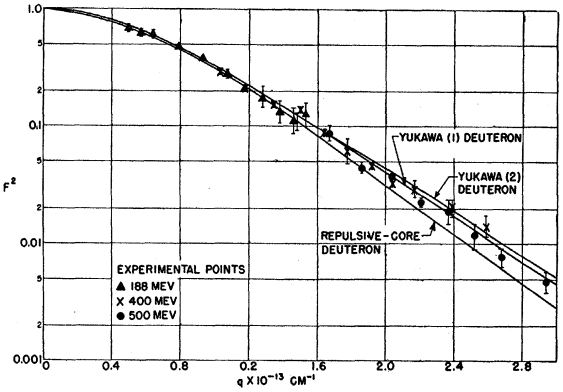

FIG. 3. The same results as in Fig. 2, except that allowance has been made for the finite proton size both in the theoretical curves, and in obtaining the experimental points from the ratio of deuterium scattering to hydrogen scattering.

It is customary to quote as the radial parameter the root-mean-square (rms) radius, $\langle r^2\rangle^{\frac{1}{2}}$. It is significant as being the first size-dependent parameter to enter in an expansion of F in terms of q:

$$F(q)=1-(1/6)q^2\langle r^2\rangle+\cdots. \tag{4}$$

For given experimental conditions the amount of information obtained depends roughly on the maximum value of $q\langle r^2\rangle^{\frac{1}{2}}$ attained. Hence more information is obtained by going to larger q, and for the same q one obtains relatively more accurate radii for larger nuclei (although the amount of detail seen will be the same).

The information given by the experiments is the form factor $F(q)$ for a range of values of q with both a maximum and a minimum q value. It would be useful to have a direct and unique measurement of $\langle r^2\rangle^{\frac{1}{2}}$ by fitting to experiments in the region where q is small enough that approximation (4) is adequate. For this it would be necessary to know the absolute cross sec-

[19] See reference 18 and Yennie, Lévy, and Ravenhall, Revs. Modern Phys. **29**, 144 (1957).

tion accurately, and in the past it has not been possible to measure it with anything like the accuracy of the relative cross section at various angles. Even supposing that the absolute cross section is available, one is with this approach looking for the nuclear finite size where it is a relatively small effect, so that a given experimental accuracy will not allow us to determine $\langle r^2\rangle^{\frac{1}{2}}$ with the same precision as is obtained in other radial parameters by fitting at larger q values.[20] Thus even at the lower energies it has seemed a more profitable procedure to assume a given form for $\rho(r)$ (and usually other knowledge of nuclei has been a reasonably close guide in this choice) and to fit the *shape* of the resulting form factor to the experimental results. We use any experimental knowledge of absolute cross sections as separate, subsidiary evidence. We are usually dealing with large enough q values that a small change in the radial parameters involved will produce considerable changes in the magnitude or shape of the form factor, so that the radial parameters can be determined quite accurately. If a number of similar shapes are used, it is usually found that $\langle r^2\rangle$ is not the same for all of them. With this method of fitting, however, this is not surprising, since $\langle r^2\rangle$ is then a derived quantity not directly measured.

This method is open to the objection that knowledge of the form factor over only a limited range of q does not determine $\rho(r)$ uniquely. Besides the pathological cases, of which there may be many, there is always the chance that different but physically reasonable ones are missed. It is certainly not always easy to see in any detail what are the common features of the various good fits to the data. Moreover, the high fourier components of the types of charge distribution we usually need to use are not always obviously related to their prominent spatial features.

With these limitations on the scope of the analysis in mind, we consider the comparison between experiment and theory for helium as shown in Fig. 4. The experiments clearly rule out extreme shapes like uniform or exponential, and are fitted quite well, both at 180 Mev and at 400 Mev, by a Gaussian shape with $\langle r^2\rangle^{\frac{1}{2}}=1.61\times10^{-13}$ cm.[1] Because of the restricted values of $q\langle r^2\rangle^{\frac{1}{2}}$ it is not profitable to consider more complicated shapes.

There are other experiments which give information about the size of this nucleus; the bremsstrahlung-weighted photodisintegration cross section measures a mean radius directly,[21] and high-energy photodisintegration gives a mean square momentum which can also be related to it.[22] These predict a radius significantly smaller than the charge radius obtained above, but as we expect from the analysis of scattering from the deuteron, they are brought into complete agreement if the finite proton size is unfolded from the charge distribution.

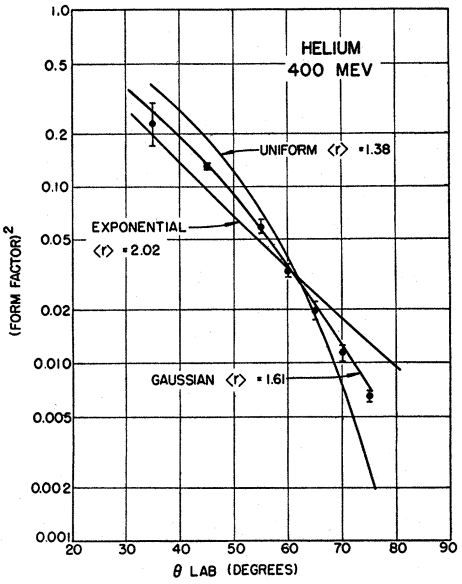

FIG. 4. Experimental and theoretical results for helium at 400 Mev, expressed as $|F(q)|^2$ *vs* scattering angle. The charge distribution used to obtain the theoretical curves are the simple one-parameter shapes; uniform, exponential and Gaussian. The rms radii indicated are in units of 10^{-13} cm.

These particular cases make it clear that in general, electron scattering measures a charge distribution which is somewhat larger than the distribution in space of the centers of mass of the nucleons. It is the latter quantity that is of interest for comparison with nonrelativistic nuclear theory, and with most other measurements. The relative effect is of course largest for the lightest nuclei, but in all cases it should be allowed for. It is easy to calculate in most cases. Of necessity, the assumption is made that the nuclear binding does not distort the free nucleon structure. With this assumption there is good agreement between experiment and nuclear theory, although neither of them is accurate enough to test it very stringently, as yet.

We have not mentioned any theory of the alpha particle structure. The usual type of variational calculation with assumed two-body forces[23] gives too small a radius by about 40%; the same conclusion, to a lesser extent, holds for He^3 and H^3, the radius in that case being inferred from the Coulomb energy. It is very plausible to suppose that this is due to neglect of repulsive cores

[20] Up to the term in q^4, $F(q^2)\cong1-(1/6)q^2\langle r^2\rangle+(1/120)q^4\langle r^4\rangle$. Because $\langle r^4\rangle$ is always greater than $\langle r^2\rangle^2$, the q^4 term in this expression is always greater than $(3/10)[(1/6)q^2\langle r^2\rangle]^2$. In order for it to be less than 5% of the q^2 term, we must have $(1/6)q^2\langle r^2\rangle<1/6$, so that $|F(q^2)|^2$, the experimentally measured quantity, must be greater than 3/4. To determine $\langle r^2\rangle$ to within 6%, $|F(q^2)|^2$ must therefore be measured to within 2%, and correspondingly for better accuracy.

[21] M. L. Rustgi and J. S. Levinger, Phys. Rev. **106**, 530 (1957); L. L. Foldy, Phys. Rev. **107**, 1303 (1957).

[22] M. Q. Barton and J. H. Smith, Phys. Rev. (to be published); and J. H. Smith (private communication).

[23] J. Irving, Proc. Phys. Soc. (London) **A66**, 17 (1953); A. C. Clark, Proc. Phys. Soc. (London) **A67**, 323 (1953).

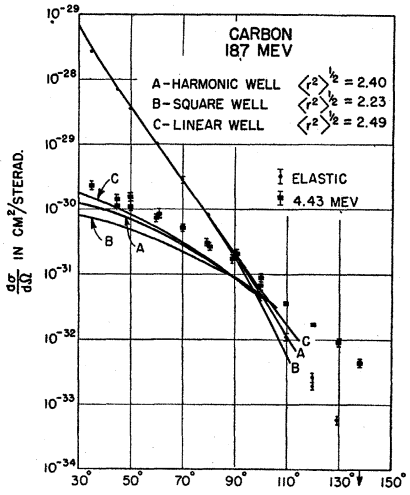

FIG. 5. Differential cross sections for scattering by carbon at 187 Mev. The theoretical curves are calculated using the Born approximation with a correction for the change in electron wave number near the nucleus. They are not continued beyond 90° because the approximation is not reliable for larger angles. The steeply falling curves are for elastic scattering, the others represent inelastic scattering associated with the excitation to the 4.43 Mev level. The three theoretical curves are calculated using the nuclear shell model, and assuming a common potential well which is square, parabolic (harmonic), or linear. The absolute scale on the latter curves is for pure $L-S$ coupling, for which the cross sections are a maximum.

in the assumed two-body force, but this belief has yet to be substantiated by an actual calculation.[24]

$1p$-shell Nuclei

The most extensive experimental results, and consequently the most elaborate analysis, have been obtained for *carbon-12* and *oxygen-16*. The experimental cross section for carbon at 187 Mev[25] is similar in character to those for helium, decreasing rapidly but smoothly over a wide angular range. The simple analytic shapes

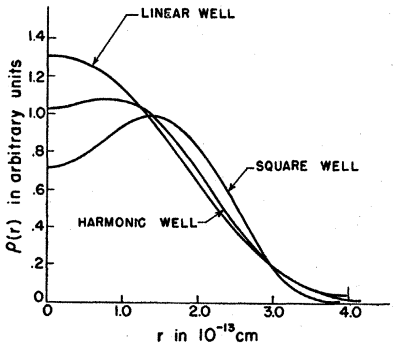

FIG. 6. Charge distributions for the shell model, in carbon, for the same three well shapes as in Fig. 5.

[24] A calculation of this kind has been made for He^3 and H^3 by Kikuta, Morita, and Yamada, Progr. Theoret. Phys. (Kyoto) **15**, 222 (1956), and they do obtain the correct Coulomb energy difference.

[25] J. H. Fregeau, Phys. Rev. **104**, 225 (1956).

for $\rho(r)$, such as uniform and exponential, and even the gaussian, do not fit very well; the accuracy and angular extent of the results now contains more information than can be expressed in those terms. While a possible approach is to introduce more complicated shapes, with more adjustable parameters, an interesting alternative is to make the analysis in terms of the nuclear shell model, and to see to what extent the assumptions made in it are consistent with the electron-scattering results.

If the ground state of the nucleus is made up entirely of the lowest configuration $(1s)^4(1p)^{2Z-4}$ the sum of $|\psi(r)|^2$ for the protons, which is what is needed for the charge distribution, is independent of the mode of coupling in the shell model, and depends only on the shape of the common potential well. Many authors[26] have pointed out that the charge distribution obtained from the (infinite) harmonic well,

$$\rho(r)=\rho(0)[1+(Z-2)r^2/3a^2]\exp(-r^2/a^2), \quad (5)$$

can, with the appropriate choice of the adjustable length parameter a associated with this well, give very good agreement with experiment. Fig. 5 shows that the agreement is significantly better than is obtained from the extreme well shapes such as the square or

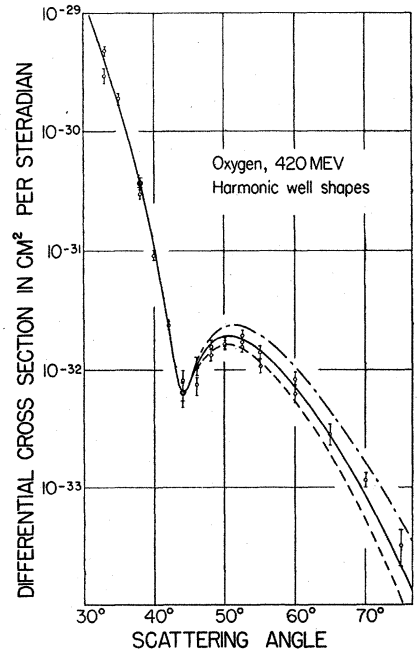

FIG. 7. Differential ions sections for scattering by oxygen at 420 Mev. All of the theoretical curves are for the harmonic-well version of the shell model, the dashed curve with no modifications. The dotted curve contains the effect of the finite proton size, and both this and the center-of-mass correction to the shell model are included in the full curve.

[26] G. Morpurgo, Nuovo cimento **3**, 430 (1956); R. A. Ferrel and W. M. Vischer, Phys. Rev. **104**, 475 (1956); M. K. Pal and S. Mukherjee, Phys. Rev. **106**, 811 (1957).

linear well.[27] This wide variation in well shapes produces much less variation in the wave functions, so that in these three cases the actual charge distributions are surprisingly similar (Fig. 6).

Some new experiments on carbon and oxygen, at 420 Mev,[28] extend to considerably larger q values, yet they are still in remarkably good agreement with the simple, harmonic-well version of the shell model. The form factor for the charge distribution (5) is

$$F(q)=\{1-[\alpha/2(2+3\alpha)]q^2a^2\}\exp(-q^2a^2/4), \quad (6)$$

where α is the factor $(Z-2)/3$ (proportional to the number of protons in the $1p$ shell). The carbon results have a pronounced diffraction minimum at the angle predicted by (6), with the value of a deduced from the 187 Mev experiments.[25] To obtain the cross section in this angular region accurately it is necessary to use the partial wave analysis. The curve fitting is now very simple: for each nucleus there is only one free parameter, a, which is fixed by the position of the diffraction minimum [as given approximately by (6)]. The very good agreement with experiment over the whole angular range, shown in Fig. 7, is then a significant confirmation of this model. There are two improvements to be made to the simple theory; inclusion of the finite proton size[29] (since the shell model presumably predicts the distribution in space of the centers of mass of the nucleons), and allowance for the fact that the shell model describes a system without a fixed center of mass.[30] In oxygen the curve which includes both of these effects, and presumably therefore, the most complete one, gives the best agreement with experiment. For carbon (Fig. 8) this result is not so clear; the cross section in the interesting region is about ten times smaller than in the corresponding region in oxygen, and so cannot be obtained as accurately. The length parameters for the two nuclei are significantly different, preliminary values being $a_C=1.60\times10^{-13}$ cm, $a_O=1.72\times10^{-13}$ cm. The parameter $[(5/3)\langle r^2\rangle]^{\frac{1}{2}}$ is, however, $1.30A^{\frac{1}{3}}\times10^{-13}$ cm for both nuclei, very close to its value for nuclei in the region of Ca^{40}. The charge distributions are illustrated in Fig. 9. It is difficult to say whether the dip in the center of the oxygen distribution is real; with the shape (5), the behavior of $\rho(r)$ in the center is tied to its behavior in the outer region of the nucleus, and it is mainly the latter parts which determine the scattering. This particular model has too few adjustable parameters to investigate this point.[31]

Other two-parameter charge distributions, of the type used in the analysis of the results for heavier nuclei, are, when fitted to the oxygen results, very similar in over-all shape to the harmonic well distribution, although none we have tried fit the data so well that shape does. The process of including more adjustable parameters so as to obtain closer fits to experiment can be carried further and rapidly becomes very in-

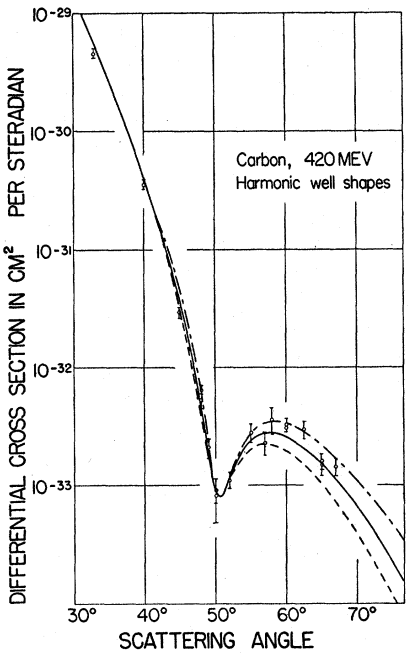

FIG. 8. Differential cross sections for scattering by carbon at 420 Mev. The theoretical curves are for the same cases as in Fig. 7.

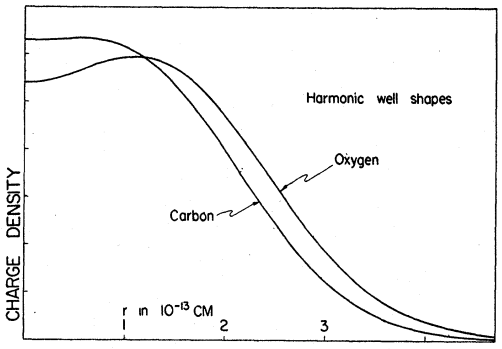

FIG. 9. Charge distributions in oxygen and carbon, corresponding to curves (3) of Figs. 7 and 8. (The carbon distribution differs a little from that shown in Fig. 6 because the latter did not include the effects of finite proton size and center-of-mass motion in the shell model.)

[27] See Sec. B of reference 25.

[28] Hofstadter, Ehrenberg, Meyer-Burkhout, and Sobottka (private communications); Ehrenberg, Meyer-Burkhout, Hofstadter, Ravenhall, and Sobottka, Bull. Am. Phys. Soc. Ser. II, 2, 390 (1957).

[29] This can be done by using the relation $F_{\text{charge}}=F_{\text{c.m.}}\times F_{\text{proton}}$. With the assumption of a Gaussian shape for the proton, F_{charge} differs from (6) only by having $a^2_{\text{c.m.}}$ replaced by $a^2_{\text{c.m.}}+a^2_{\text{proton}}$ in the exponent, so that computationally the problem is as simple with F_{charge} as with (6).

[30] C. Schwartz (private communication). The main effect is to insert in the exponent of (6) a factor $1-(1/A)$, so that the computation is just as simple as with (6).

[31] D. L. Hill reported at the Stanford Conference that he and K. Ford have analyzed the carbon experiments using a three-parameter charge distribution, and find the best fit to have no dip in the center.

volved. Guidance from nuclear theory as to the significant features to look for is very desirable.

Inelastic Scattering

The measurements on carbon, and on a series of light nuclei, have included differential cross sections for inelastically scattered electrons, corresponding to excitation of the nucleus to its low-lying levels.[25,32] The angular distribution in this case is another indication of nuclear size and shape.[33]

The process is Coulomb excitation, with some simplifying features. The differential cross section in Born approximation is almost identical with the expression for elastic scattering; the difference is that the form factor is now the Fourier transform of the *transition* charge density. Thus for a transition of known multipolarity, one can learn from electron scattering the strength of the transition [corresponding to $F_e(0)$] and the radial dependence of the transition density. From the latter we can extract the radial character of the excited state. For example, as illustrated in Fig. 5, from the cross section associated with excitation of the 4.43-Mev level in carbon, an $E(2)$ transition, it is possible to verify the conclusion obtained from elastic scattering that the well is close to harmonic, although the strength is rather difficult to fit.[27]

For such measurements to be possible it is usually necessary to have resolvable levels, and this is a rather stringent restriction on the nuclei that can be examined. A useful exception is scattering from distorted nuclei, which with present resolution includes elastic scattering and inelastic scattering corresponding to excitation of the rotational levels. A sum rule for these processes allows the scattering to be expressed simply in terms of the intrinsic deformation of the nucleus.[33] It is then possible to learn something about the radial character of this deformation, as well as to measure the distortion parameter.[34]

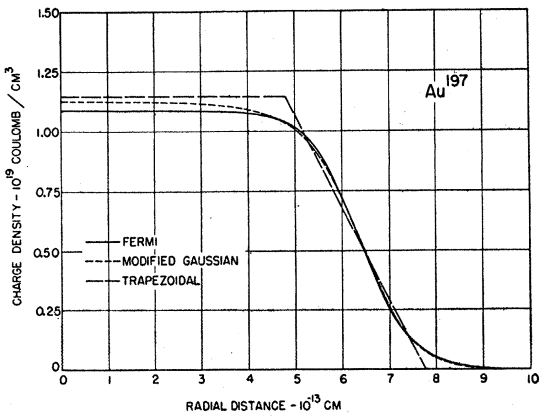

FIG. 10. Three two-parameter charge distributions in gold. Each is the best fit to the 183 Mev experiments of a particular functional form for $\rho(r)$. Reference 35 gives definitions and parameters.

[32] R. Helm, Phys. Rev. **104**, 1466 (1956).
[33] L. I. Schiff, Phys. Rev. **96**, 765 (1954).

Both types of inelastic scattering require calculations more accurate than the simple Born approximation. The partial wave analysis works only for spherically symmetric charge distributions, so that some approximate methods must be used. The modified Born approximation described in Sec. II can probably be made accurate enough to do this.

Larger Nuclei[35]

The early results on nuclei from Ca^{40} to Bi^{209} have not been added to recently.

The nuclei examined are believed to be spherically symmetric. The differential cross sections show diffraction structure characteristic of charge distributions which are roughly uniform, with a smoothed edge; this is also about all that current nuclear theory can say, so that we can get no further guidance from it. The more numerous experimental results on Au^{197} were examined closely to find the amount of detail detectable in the shape of the surface, and to investigate a possible smooth variation of charge density in the inner region. The results are best expressed pictorially. Figure 10 shows three different surface shapes, one with an exponential tail (Fermi shape), one with a gaussian tail, and one with no tail at all, all of which fit the experiments equally well, and so are not distinguishable. The allowable variation in central density is illustrated in Fig. 11, and it is rather wide. The conclusion drawn was that variation in central density was too fine a feature to be detectable in those experiments, and that the only property of the surface that could be measured was its thickness (best characterized by t, the 90% to 10% distance) and not its detailed shape. Consequently, while for convenience the results on the other nuclei were analyzed in terms of the Fermi shape

$$\rho(r)=\rho_0[1+e^{(r-c)/z_1}]^{-1},$$

the only significant quantities determined were the radius and the surface thickness t. The radial parameter c, the distance to the point where ρ has dropped to half of its central value on this model, varies closely as $A^{\frac{1}{3}}$ for all of the nuclei, and t is effectively constant:

$$\left.\begin{aligned} c&=(1.07\pm0.02)A^{\frac{1}{3}}\times10^{-13}\text{ cm}\\ t&=(2.4\pm0.3)\times10^{-13}\text{ cm}\end{aligned}\right\}\begin{matrix}\text{charge}\\ \text{distribution.}\end{matrix}$$

[34] Downs, Ravenhall, and Yennie, Phys. Rev. **106**, 1285 (1957).
[35] The results described are those of Hahn, Ravenhall, and Hofstadter, Phys. Rev. **101**, 1131 (1956). Analyses of the experiments on gold have been made also by Hill, Freeman, and Ford (reference 3) and Brown and Elton (reference 12). To the extent that the results of the various groups overlap there is substantial agreement, although Hill, Freeman, and Ford find certainly no appreciable central dip in the gold distribution. Since all of the groups are analyzing Hofstadter's data, their somewhat different conclusions on this point from Hahn *et al.* may be due to slightly different criteria for least-squares fitting.

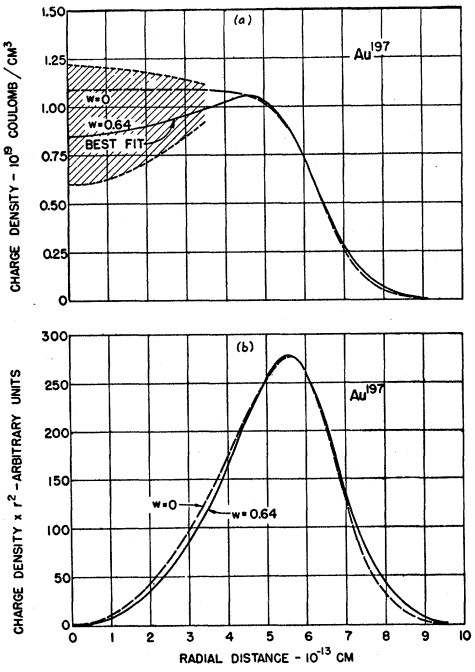

FIG. 11. The best fit to the gold experiments using a three-parameter charge distribution which has an exponential tail and a variable central density. Also shown are the allowable variation in central density, and the Fermi two-parameter best fit of Fig. 10 (labeled $w=0$).

The analysis of less detailed experiments on lighter nuclei (Mg, Si, S) using a corrected Born approximation[32] gives radii in agreement with this value. We must remember that the distribution in space of the centers of mass of the protons is slightly different from the charge distribution because of the finite proton size. For these large nuclei the effect on the radius is small, but on the surface thickness it is quite appreciable[36]:

$$\left.\begin{aligned} c&=(1.08\pm0.02)A^{\frac{1}{3}}\times10^{-13}\text{ cm}\\ t&=(2.2\pm0.3)\times10^{-13}\text{ cm}\end{aligned}\right\}\begin{aligned}&\text{center of mass}\\&\text{distribution.}\end{aligned}$$

The often-quoted radial parameter $R=[(5/3)\langle r^2\rangle]^{\frac{1}{2}}$ (the radius of the uniform distribution having the same rms radius) does not vary exactly as $A^{\frac{1}{3}}$; it decreases from $1.32A^{\frac{1}{3}}\times10^{-13}$ cm for Ca^{40} to $1.20A^{\frac{1}{3}}\times10^{-13}$ cm for Bi^{209}.

The apparent, although now familiar, smallness of c compared with previous knowledge of nuclear size is due to its definition—for a shape with an extended surface it is clearly smaller than R—and to the fact that other measurements of nuclear radii, which do not distinguish anything but a radius, generally measure R rather than c.

The present results give only a radius and a surface thickness. They cannot say whether densities in the interior of the nucleus are constant, nor whether the tail of the distribution falls off in any particular way. The limitation on the conclusions is entirely due to experimental uncertainty and limitation on q values investigated. An improvement in either of these, such as is now possible, can surely improve this situation. This is demonstrated by calculations of the cross section for Au^{197} at 240 Mev[37] shown in Fig. 12. Some of the charge distributions that are indistinguishable with the present results, which covered the region through the second diffraction dip, have measurably different cross sections in the next diffraction peak. We shall soon be able to decide on points like the shape of the surface and the central dip, but the number of different ways that even these features can be introduced is very great, so that the results become somewhat arbitrary. It would be useful to have guidance from nuclear theory on such points.

As a complement to the above investigation of the over-all variation of nuclear parameters for a wide range

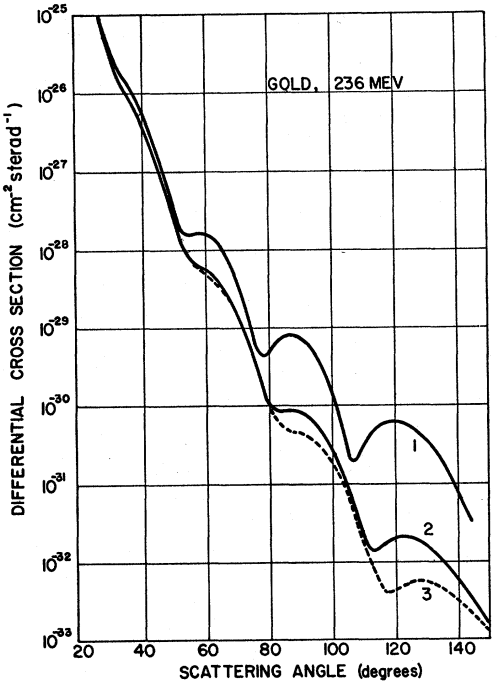

FIG. 12. Differential cross sections for scattering by gold at 236 Mev. The charge distributions are (2) the Fermi shape of Fig. 10, and (3) a three-parameter shape of the kind illustrated in Fig. 11, for $w=1.20$. The experiments at 183 Mev were not able to distinguish between these two shapes. For comparison, curve (1) is for the uniform distribution $kR=8$.

[36] These results were quoted in footnote 44 of reference 19. They can be obtained either by evaluating the folding integral $\rho_{\text{charge}}(\mathbf{r})=\int d^3r'\rho_{\text{c.m.}}(r')\rho_{\text{proton}}(|\mathbf{r}-\mathbf{r}'|)$, or by using the corresponding relation among the Fourier transforms. [The Fourier transform of the Fermi function has been given by R. Blankenbecler, Am. J. Phys. **25**, 279 (1957).] Using the former method, it is easy to show that, in terms of the parameter s, the rms surface thickness, $s^2_{\text{charge}}=s^2_{\text{c.m.}}+(4/3)\langle r^2\rangle_{\text{proton}}$, $[s^2=-4\int(r-c)^2\rho'(r)\times dr/\rho(0)$; see D. G. Ravenhall and D. R. Yennie, Phys. Rev. **96**, 239 (1954), and reference 35]. Present uncertainties in knowledge of the shape of the surface make it sufficient to use the approximation that ρ_{charge} and $\rho_{\text{c.m.}}$ have the same shape, but slightly different parameters. The results, which are insensitive to the particular features of the two distributions which are used to obtain them, are that $t_{\text{charge}}\cong1.13t_{\text{c.m.}}$, and $c_{\text{charge}}-c_{\text{c.m.}}\cong-0.13A^{-\frac{1}{3}}\times10^{-13}$ cm.

[37] D. G. Ravenhall and D. R. Yennie, Proc. Phys. Soc. (London) **A70**, 857 (1957).

of A, a method exists for looking at the fine variation of these parameters from one nucleus to the next. For nuclei which can be made up into targets of very similar chemical constitution, it is always possible to measure ratios of scattering cross sections more accurately than their absolute values, because it is possible to count the electrons coming from each target while keeping all other conditions identical. Because of the diffraction structure in the cross sections for heavier nuclei these ratios depend sensitively on small variations in radii. For instance, experiment clearly shows up[38] a 1.2% difference in radius between Ni^{58} and Ni^{60}. This method has not been exploited very much as yet.

[38] Hahn, Hofstadter, and Ravenhall, Phys. Rev. **105**, 1353 (1957).

IV. CONCLUSION

For each region of the periodic table, the appropriate approximation to nuclear theory suggests shapes that it is interesting to examine. Detailed comparison with the electron scattering experiments then allows accurate determination of some of the relevant parameters. This procedure avoids the arbitrariness of *ad hoc* inclusion of a large number of adjustable parameters, but it is limited by the specificity of the nuclear model being used. In all of the regions, hints from nuclear theory as to some of the finer features of nuclear shape, such as the form of the extreme tail of the charge distribution, would be invaluable in the extraction of more detailed information from future experiments.

REVIEWS OF MODERN PHYSICS VOLUME 30, NUMBER 2 APRIL, 1958

Nuclear Radii from Mesonic Atoms

ERNEST M. HENLEY

University of Washington, Seattle, Washington

1. INTRODUCTION: PROPERTIES OF THE μ MESON

THE history of μ-mesonic atoms stretches over almost a decade, with but little recent experimental work. The beginnings of the study of the μ-mesonic atom occurred in 1949, when Chang[1] noted that electromagnetic radiation accompanied the decay of negative μ mesons in matter. This was interpreted by Wheeler[2] as being due to γ rays both before and after capture of the meson, in about equal proportion. Wheeler made a careful analysis of the μ-mesonic atom and pointed out the usefulness of more refined measurements. This led to the experiments of Fitch and Rainwater,[3] which gave the first clear-cut evidence of the small radius of the proton distribution in the nucleus.

The μ meson in many ways is an ideal test particle of the nuclear charge distribution. Such a test particle should have no internal structure and its interaction with the nucleus should be fully understood. These requirements are almost completely satisfied by the μ meson. The main force between the μ meson and the nucleus is an electrostatic one, the nature of which is well known. Although a careful study of nonelectromagnetic forces has not yet been carried out, indications are that these are very weak. There continue to be debates on the anomalous large-angle scatterings of cosmic-ray μ mesons with nuclei,[4] but interpretation of these experiments is still not clear. Experiments performed here, at Stanford, by Masek and Panofsky[4] on the production of μ-meson pairs by high-energy electrons are difficult to reconcile with such scatterings for low-energy μ mesons (i.e., momentum transfer <200 Mev/c). I shall consider evidence for a relatively strong specific nuclear interaction of bound μ mesons as nonexistent, and I believe that this is not contrary to general experimental findings.[5] The only specific interactions are then that which produces the μ meson from the π and that responsible for the absorption of the μ meson by nucleons; these forces are 10^{-10} of the electromagnetic one in strength.

When the experiments of Fitch and Rainwater[3] were carried out in 1952, the other properties of the μ meson were not nearly as well known as they are now. Thus, the mass of the μ meson was thought to be $210m_e$ in 1952. More accurate measurements, some of which actually make use of x-rays from π- and μ-mesonic atoms and of the photoelectric K-absorption edge, have since bracketed the mass between[6]

$$206.77\pm0.04 \quad \text{and} \quad 207.1\pm0.11m_e,$$

[1] W. Y. Chang, Revs. Modern Phys. **21**, 166 (1949).
[2] J. A. Wheeler, Revs. Modern Phys. **21**, 133 (1949).
[3] V. L. Fitch and J. Rainwater, Phys. Rev. **92**, 789 (1953).
[4] For experimental work and discussion, see G. Masek and W. K. H. Panofsky, Phys. Rev. **101**, 1094 (1956).
[5] The momenta of the bound μ mesons are of the same order of magnitude as those involved in the experiment of Masek and Panofsky.
[6] Koslov, Fitch, and Rainwater, Phys. Rev. **95**, 291, 625 (1954); Cohen, Crowe, and DuMond, Phys. Rev. **104**, 266 (1956).